NaY Zeolite and TiO_2 Impregnated NaY Zeolite for the Adsorption and Photocatalytic Degradation of Methylene Blue under Sunlight

Baouali, Nazim Younes; Nibou, Djamel*[+]; Amokrane, Samira

Laboratory of Materials Technology, University of Science and Technology Houari Boumediene, B.P. 32, El-Alia, Bab-Ezzouar, Algiers, ALGERIA

ABSTRACT: *NaY zeolite was impregnated by TiO_2 to prepare a novel catalyst for the adsorption and photocatalytic degradation of methylene blue (MB). The samples were characterized by XRD, SEM, EDS, and FT-IR techniques. The percentage adsorption of MB on NaY reaches 88% and an adsorption capacity of 6.55 mg/g under optimized parameters ([MB] = 10 mg/L, pH = 6, S/L = 2 mg/L, and T = 25°C). The MB adsorption process follows Langmuir isotherm. The thermodynamic parameters were investigated and showed an endothermic and physical process. The MB adsorption also follows a pseudo-second-order kinetic. The photo-degradation of the MB dye was successfully carried out on the TiO_2/NaY catalyst under sunlight. The MB photo-degradation also follows a Langmuir-Hinshelwood first-order kinetic.*

KEYWORDS: *Adsorption; Photo-degradation; Methylene blue; NaY zeolite; TiO_2; Dye; LH Kinetic.*

INTRODUCTION

Dyes are extensively employed in the food and textile industries and represent an increasing threat to the aquatic medium [1]. Their presence in water, even at low amounts, is harmful to aquatic life since they attenuate the light flux and inhibit photosynthesis and in a way aquatic life [2]. Dyes are primarily of synthetic origin and possess complex structures, which make them stable to both light and heat. Therefore, it is necessary to remove them before their discharge into water [3].

The treatment of colored water is actively investigated and the topic continues to attract great interest from environmental researchers [4-9]. The classical and nonclassical methods for the removal of the dye include coagulation, electrochemical conversion, extraction, and advanced oxidation [5-7]. However, some of these methods are efficient for low pollutants concentration as adsorption while others are efficient for the highly concentrated state as coagulation-filtration.

So, other strategies for wastewater treatment must be used [8-9] and adsorption is found to be attractive because of its simplicity. Advanced Oxidation Process (AOPs) is also suitable for the degradation of hazardous pollutants by radicals $OH^{\bullet}$ and/or $O_2^{\bullet}$ which are able to oxidize organic compounds into water, carbon dioxide, and inorganic ions [10,11]. In this respect, photocatalysis appears as an attractive technology because of the clean and inexhaustible energy of the sun[12-14]. Accordingly, the zeolites [15-19], clays [20-21], bio-adsorbents [22-23]

** To whom correspondence should be addressed.*
+ E-mail: dnibou@Yahoo.fr ; djamelnibou@gmail.com ; dnibou@usthb.dz
1021-9986/2022/6/1907-1920 14/$/6.04

and activated carbons [24-25] are currently favored adsorbents and can efficiently remove pesticides, organic compounds, and heavy metal ions such as iron, nickel, zinc, lead, chromium, and uranium. Catalytic materials based on NaY zeolite occupy a very important place in heterogeneous catalysis [26-31].

The NaY is known as an aluminosilicate with a framework composition based on tetrahedra SiO_4 and AlO_4^-. The negative charge of the structure is neutralized by a positive mental charge M^+ and is also known as the exchangeable ion metal [32-35]. NaY is a suitable choice for adsorption ions and organic compounds due to its high ion exchange capacity and high volume porosity. Its super cages with aperture (7.5 Å) and diameter (12.5 Å) [32, 36] are able to fix and adsorb heavy ions and organic molecules as dyes.

In the present work, we have approached the problem first on the adsorption side and then by catalytic oxidation of the MB by adsorbent-catalysts TiO_2/NaY, specific features of NaY zeolite such as transparency to sunlight allow penetration into the solid opaque powder to reach the substrate molecules located inside particles [37].

Methylene Blue (MB) is a model dye extensively used in the textile industry and is very soluble in water (44 mg/L at 25°C). MB dye can affects both the ecosystem and human health. At strong used doses, MB dye can be highly toxic, and carcinogenic, irritating affected tissues, abdominal and pericardial pain, dizziness, headache, profuse sweating, and mental confusion [1, 6].

The main purpose of the present study is to investigate the performance of the NaY zeolite and TiO_2/NaY through successive processes for the adsorption/photocatalysis of MB. The effect of catalyst dose, solution pH, initial MB concentration and temperature for the adsorption/photodegradation are investigated on the NaY zeolite and TiO_2NaY respectively.

EXPERIMENTAL SECTION

Catalyst preparation

TiO2 /NaY was prepared by a known method [37] by dispersing 1 g of TiO_2 (from Degussa) and 3 g of NaY zeolite (purchased from Linde) in 200 mL of distillate water. The mixture is left under stirring for 8 h at a temperature of 25°C and dried at 80°C to remove water. Finally, the obtained powder is calcined in an oven at 300 °C for 6 h to assure the incorporation of TiO_2 onto NaY zeolite.

Characterization

NaY zeolite, TiO_2, and TiO_2/NaY were identified with a Philips PW 1800 diffractometer, using CuKα radiation (λ= 0.15418 nm), at a scan range 2θ from 5 to 120°. The morphology of the catalysts was studied by scanning electron microscopy (SEM) using a JEOL, JSM-6360LV microscope. The samples were also characterized by FT-IR using a Philips PU 9800 apparatus in the scan range ν from 4000 to 400 cm^{-1}.

Batch experiments and photocatalytic tests

MB is an azo dye characterized by medium toxicity and weak biodegradability. The adsorption and photocatalytic tests were done in batch mode using 250 mL of MB solution at different concentrations (10-120) ppm. The pH (3, 4, 6, 8, and 10) was adjusted by dropwise addition of acid or basic solutions. The dispersion of the powder was carried out by magnetic stirring at 400 rpm and for 60 min to reach the equilibrium state in the dark. Then, the system was exposed to solar illumination. The aliquots were taken at regular time intervals and subjected to strong centrifugation (2000 rpm, 20 min) to remove the solid particles. The disappearance of MB was followed by UV-Visible spectrophotometry (Shimadzu UV1800, λ_{max}= 665 nm) using 1 cm quartz cell. The conversion yield is determined from the relation:

$$(\%)\text{Adsorption} = \frac{C_0 - C}{C_0} \times 100 \quad (1)$$

Where C_o and C are the initial and equilibrium MB concentrations (mg/L), respectively.

RESULTS AND DISCUSSION

Characterization

Fig.1(a) and (b) show the XRD patterns of TiO_2 and TiO_2/NaY catalysts which are compared and identified with those given in the collection of simulated XRD powder patterns [38]. The identification of the NaY zeolite was done according to a standard file (JCPDS 00-012-0228). The most important XRD peaks characterizing NaY zeolite appear at 2θ: 6.19°; 10.11°; 11.86°; 11.32°; 15.61°; 17.56°; 18.64°; 20.30°; 23.58°; 26.97°; 30.36° and 31.31° (Fig.1(b)). The presence of TiO_2 in the NaY zeolite structure is characterized by its XRD 2θ positions (Fig.1(a)) marked by dashed lines indicating the

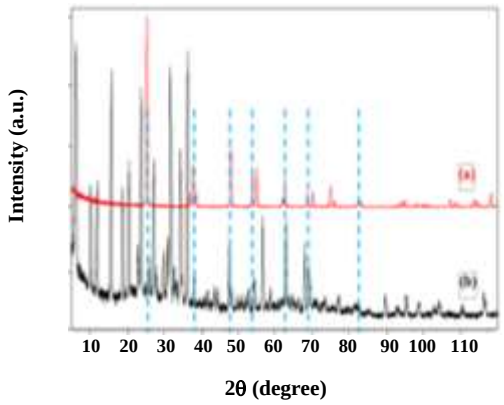

Fig. 1: XRD patterns of TiO_2 (a) and TiO_2/NaY (b).

incorporation of TiO_2 in the NaY framework structure. These results are similar to those obtained by *Tayade et al.* [37] who reported the enhanced photocatalytic activity of TiO_2 –coated NaY for degradation of MB in water; by *Shirani et al.* [39] and *Zendehdel* [40] in their works related to the removal of MB by magnetic NaY zeolite and TiO_2/NaY zeolite respectively.

Upon exploring the SEM image, a heterogeneous distribution of TiO_2 nanoparticles is detected on and around the NaY zeolites. The size of the well-defined spherical grains of the zeolite is found to be less than 2 µm under SEM observation (Fig.2(a) and (b)).

The results of the EDS analysis (Fig.2) confirm the presence of the main elements of NaY zeolite and TiO_2/NaY : (Na, Si, Al, Ti) in the structure frameworks. We note that the Si/Al ratio of NaY zeolite and TiO_2/NaY remained fixed (1.35) after doping and that the wt% of sodium has decreased (from 12.76 to 9.12) indicating that the structure is preserved and TiO_2 has been doped by the exchange process.

The NaY zeolite structure is not affected byTiO_2 loading, thus providing highly active sites which allow the dye molecules to adsorb easily onto the surface and in the way an increased photocatalytic interaction capacity of TiO_2 [37].

Fig. 3 shows the FT-IR spectra of TiO_2 and TiO_2/NaY between 400 to 3800 cm^{-1} which indicate the absorption bands of the structures. The TiO_2 spectrum (Fig. 3 (a)) is characterized only by two large bands at 710 and 503 cm^{-1}. The NaY zeolite is characterized by Si-OH hydroxyl groups in the region 3736 cm^{-1}, a large O-H-(H_2O) band at 3455 $cm^{-1,}$ and the stretching vibration of H_2O molecules at 1637 cm^{-1} was reported by *Nibou et al.* [16] and *Ferhat et al.* [18]. NaY zeolite is also characterized by the bands at 1198 and 1046.9 cm^{-1} and is attributed to the asymmetric vibration of Si-O-Al and Si-O. Other bands at 810.9, 585.1, and 455.3 cm^{-1} are assigned to symmetric stretching of Si-O-Si, Al-O, and double rings D_4 and D_6 reported by Breck [32]. The two TiO_2 bands at 710 and 503 cm^{-1} marked by dashed lines are present in the TiO_2/NaY spectrum confirming the results of XRD and EDS analysis.

Adsorption study

Effect of the pH

In order to check the pH effect on the dye adsorption, we adjusted the pH at 3, 4, 6, 8, and 10. The rate of MB adsorption for different pHs (Fig.4(a)) shows that the dye is better adsorbed in an acid medium (95%, pH 3) than in a basic solution (88% with pH 8) or neutral (86% with pH 7). Although the difference is not significant, this is due to the negative charge of the NaY zeolite in an acidic medium, which promotes the adsorption of MB (cationic dye) by electrostatic attraction [39].

The point of zero charge pH_{pzc} (Fig.4 (b)) corresponds to a zero surface charge. At low pHs ($<pH_{pzc}$), the zeolite surface is positively charged, thus attracting cations/repelling anions [9, 11, 18].

The maximum adsorption percentage at lower pH may be due to the electrostatic attractions between negatively charged functional groups of the MB dye and the positive charge of the NaY zeolites surface [40]. Hydrogen ions also act as a linking ligand between the NaY and MB molecules dye. At high pH, the NaY acquires a negative charge and no hydrogen bonds can be formed between MB and NaY surface, and then only Van der Waals forces contribute to MB adsorption.

Effect of contact time

The enhanced MB adsorption is attributed to the fact that initially, all sites on the adsorbent surface are available and the gradient of MB concentration is high. Accordingly, the extent of MB uptake decreases over time, due to the decrease of vacant sites. The remaining internal sites become difficult to be occupied because of the repulsive forces between the MB molecules on the zeolite surface and the bulk phase, thus leading to the saturation state [41].

The MB adsorption onto NaY makes it possible to determine the adsorption equilibrium time or the saturation

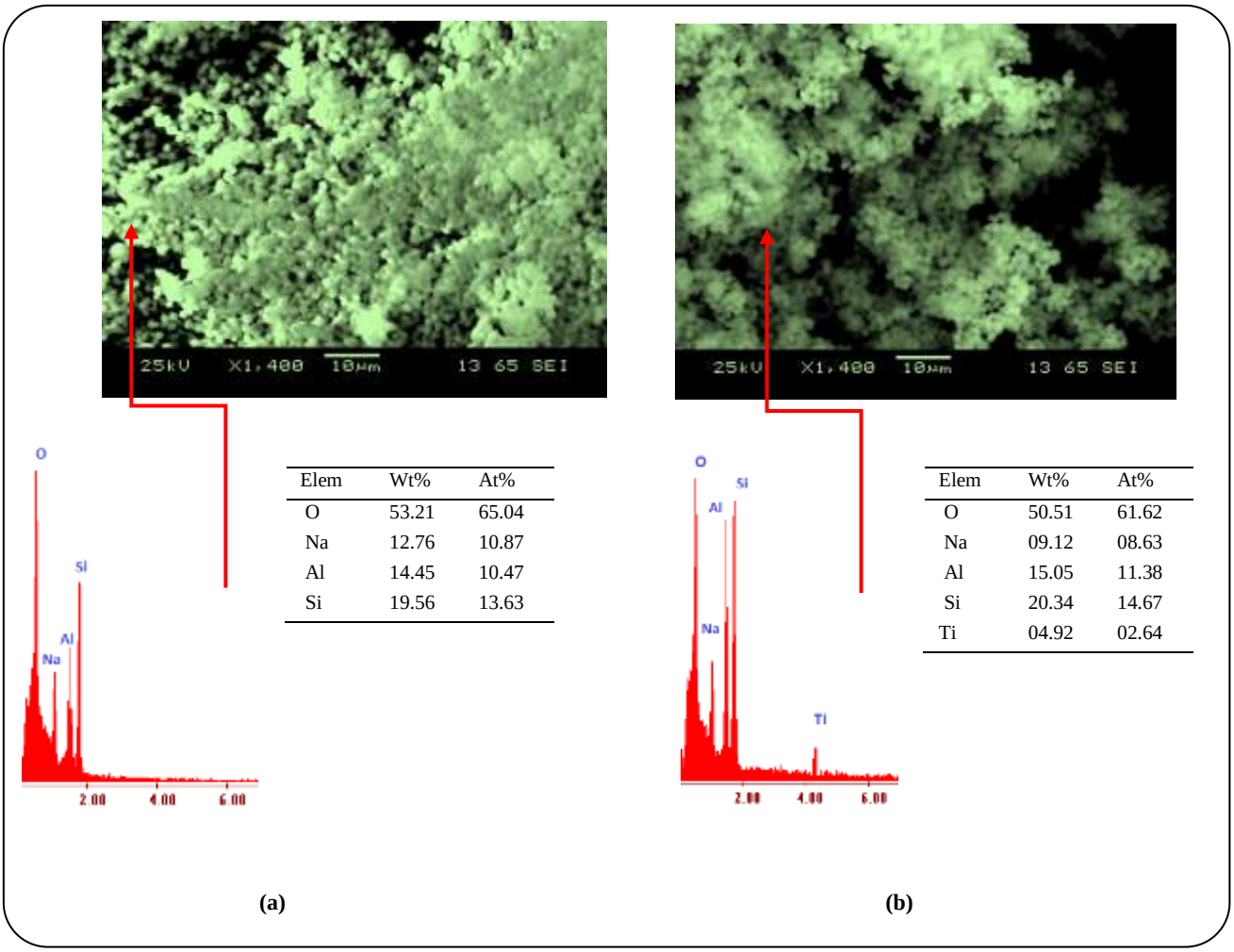

Elem	Wt%	At%
O	53.21	65.04
Na	12.76	10.87
Al	14.45	10.47
Si	19.56	13.63

Elem	Wt%	At%
O	50.51	61.62
Na	09.12	08.63
Al	15.05	11.38
Si	20.34	14.67
Ti	04.92	02.64

(a) **(b)**

Fig. 2: SEM micrographs observation and EDS analysis of NaY(a) and TiO_2/NaY (b).

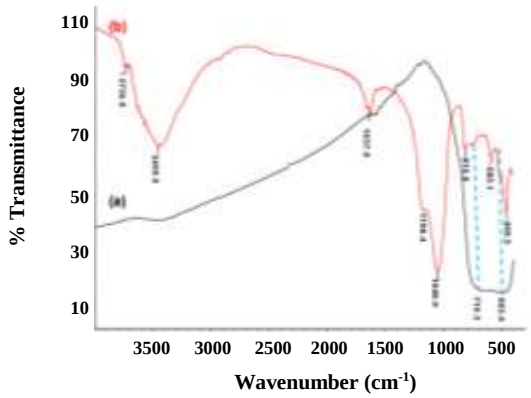

Fig. 3: FT-IR spectra of TiO_2 (a) and TiO_2/NaY (b).

point of zeolite by the dye. According to the results reported in Fig.5, we noticed that 30 min of contact with NaY zeolite is needed to reach the equilibrium time.

Increasing the contact time enhances the adsorption but with an irregular shape. This is due to the difficulty of MB molecules reaching the inside pores of the NaY zeolite because of the saturation of active sites on the surface. Therefore, the adsorption remains almost constant over time. This is due to the occurrence of molecule transfer ascribed to MB-adsorbent interactions with neglected interaction solute-solute.

Effect of solid/liquid ratio and the initial MB concentration

The aim of this section is to determine the optimal quantity of NaY zeolite for different solid-liquid ratios necessary to absorb the maximum of MB. Fig.6 (a) shows that for the same MB concentration, the adsorption rate increases proportionally with the solid/liquid ratio. The contact surface induced a greater availability of increasing adsorption sites for fixing the MB molecules;

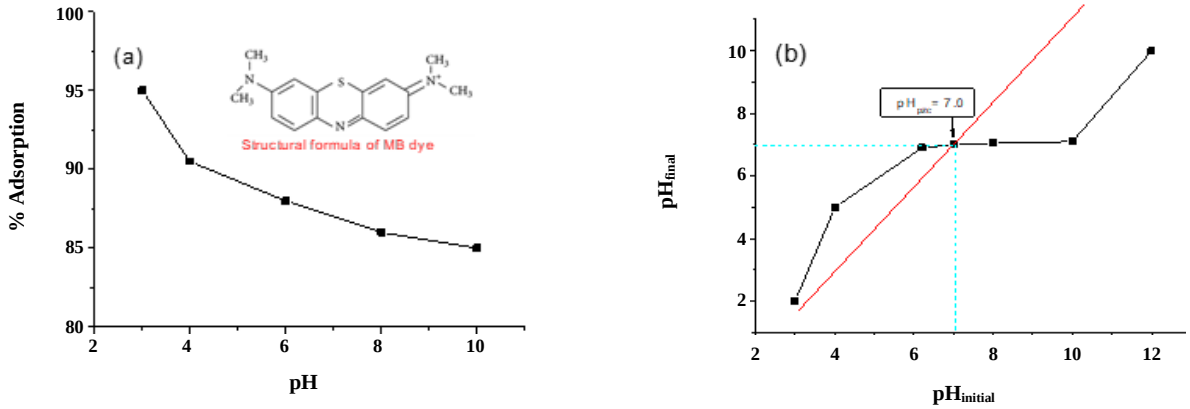

Fig. 4: (a) Effect of the pH on MB adsorption onto NaY zeolite ([MB] = 10 mg/L, S/L = 2 g/L and T = 25°C). (b) Point of zero charges of NaY.

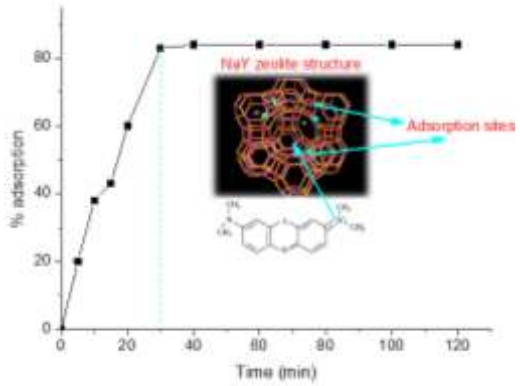

Fig. 5: Effect of the contact time on MB adsorption onto NaY zeolite ([MB] = 10 mg/L, S/L = 2 g/L, pH = 6 and T = 25°C).

similar results were found elsewhere [42].

MB is an organic pollutant and its concentration represents an important parameter in wastewater treatment. Effluents are thrown into the aquatic medium in various quantities and it is interesting to study the dye elimination by varying the MB concentration (C_o) in the range (10–100 mg/L) at room temperature keeping the other parameters constant. Fig.6 (b) shows that the adsorption percentage of MB increases with decreasing the concentration C_o indicating that fewer favorable sites become involved when the MB solution concentration is high [43].

Effect of temperature on the MB removal

Temperature is one of the crucial factors in the adsorption of the dye. To study the thermal effect on the MB adsorption process, we retained four temperatures: 23, 40, 50, and 60°C. Fig.7(a) shows that the evolution of the adsorption rate increases with raising the temperature. The rate increases from 84% at 22°C and reaches 93% at 60°C; above this temperature water vaporization becomes important. The thermal variation stimulates the movement of the molecules which increases their mobility, thus improving the adsorption process [40].

The increase of the adsorption with temperature is attributed to either an increase in the number of available sites for sorption on the adsorbent [42, 44] or to the decrease in the boundary layer thickness surrounding the dye, so that the mass transfer resistance of the adsorbate in the boundary layer decreases.

Thermodynamic parameters

The thermodynamic parameters provide additional in-depth information regarding the inherent energetic changes involved during MB adsorption. The standard enthalpy change (ΔH°), entropy change (ΔS°), and free energy change (ΔG°) are evaluated from the equation:

$$\ln K_c = \frac{\Delta S^0}{R} - \frac{\Delta H^0}{RT} \quad (2)$$

$$K_c = \frac{(C_0 - C_e)}{C_e} \quad (3)$$

Where K_c is the equilibrium constant.

$$\Delta G^o = \Delta H^o - T\Delta S^o \quad (4)$$

ΔH^o and ΔS^o values can be obtained from the slope and the interception of the ln K_c plot as a function of (1/T)

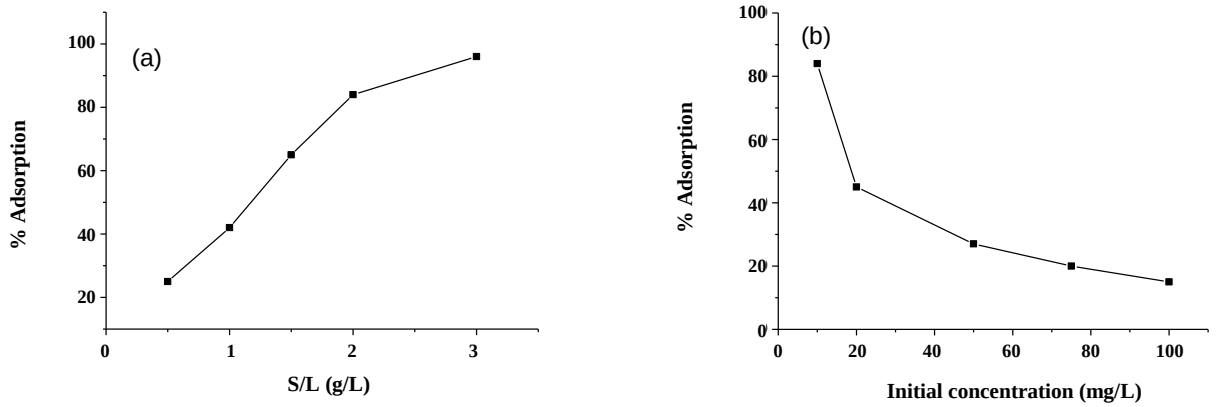

Fig. 6: (a) Effect of the S/L ratio on MB adsorption onto NaY zeolite ([MB] = 10 mg/L, pH = 6 and T=25°C) and (b) Effect of the initial MB concentration on adsorption onto NaY (S/L = 2 g/L, pH = 6 and T=25°C).

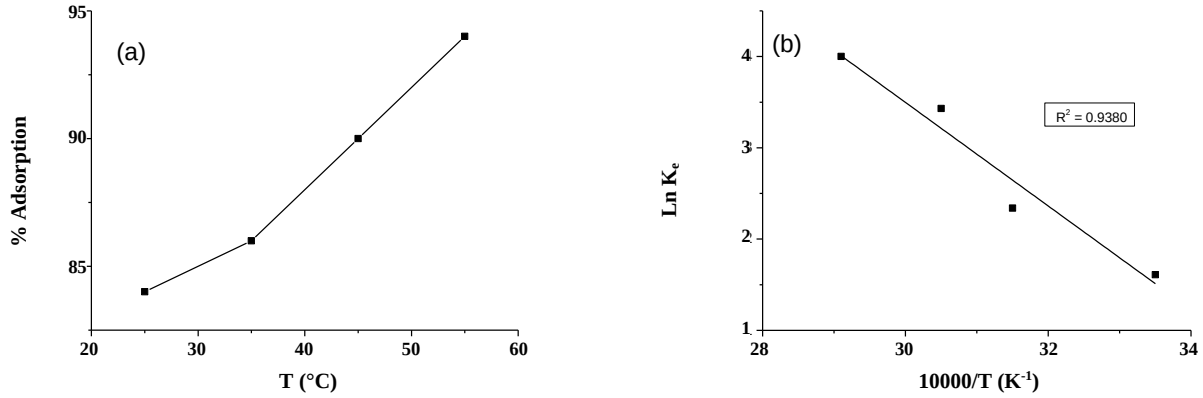

Fig. 7: (a) Effect of the temperature on MB adsorption onto NaY zeolite and (b) Variation of ln K_c as a Function of (1/T) ([MB] = 10 mg/L, pH = 6 and S/L = 2 g/L).

(Fig.7(b)). The thermodynamic parameters are listed in Table 1. The positive value of ΔH° confirmed that the adsorption of MB is an endothermic process. The negative value of ΔG° decreases with raising the temperature, indicating the spontaneity of the MB adsorption while the positive ΔS° showed an increase in the randomness at the solid/solution interface and the affinity of the adsorbent material NaY toward MB [45]. Similar results were reported for MB adsorption on different adsorbents [46].

According to the magnitude of ΔH°, the adsorption process can be classified as physical (ΔH°<84 kJ/mol) or chemical (84–420 kJ/mol) [47]. It is clear that MB adsorption onto NaY zeolite is physical.

Adsorption equilibrium.

The equilibrium isotherms permit for understanding the adsorption mechanisms and various models have been used for the MB adsorption onto NaY zeolite under the following conditions: S/L = 2 g/L, [MB] = 10 mg/L, pH = 6, and contact time = 30 min.

The adsorption isotherms describe how the adsorbate interacts with the adsorbent. An adsorption isotherm is characterized by constants that express the surface properties and affinity of MB and can also be used to compare the adsorption capacity of the zeolite for different pollutants. For this purpose, we have applied the known isotherms namely Langmuir, Freundlich, and Temkin [20].

The Langmuir isotherm model is commonly used to quantify the amount of adsorbate on the adsorbent as a function of the dye concentration at a given temperature. It suggests that the uptake occurs on a homogeneous monolayer surface with no interaction adsorbed/molecule. The linear form of the model is given by:

Table 1: Thermodynamic Parameters for adsorption of MB on NaY zeolite.

		ΔG° (kJ/mol)			
ΔH° (kJ/mol)	ΔS° (J/mol K)	298 K	313 K	328 K	343K
46.9741	0.1747	- 3.8162	- 6.3728	- 8.9293	- 11.4859

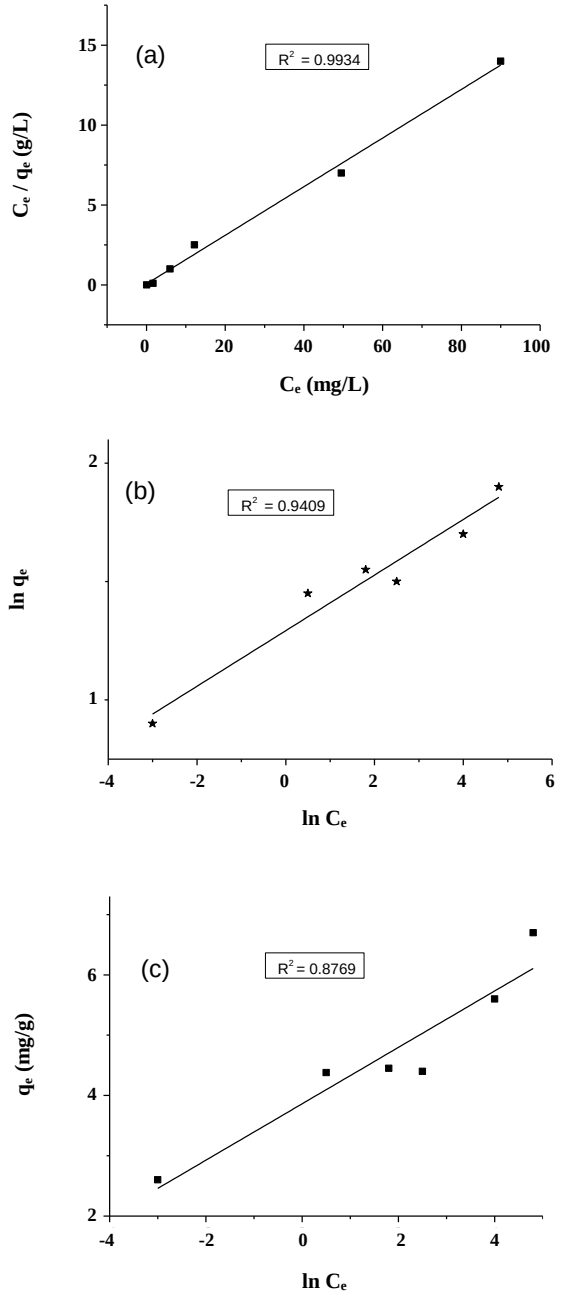

Fig. 8: MB adsorption isotherms for the MB adsorption onto NaY. (a): Langmuir, (b): Freundlich and (c): Temkin (S/L = 2 g/L, pH = 6, C_o = 10–100 mg/L and T = 25°C).

$$\frac{c_e}{q_e} = \frac{1}{q_m b} + \frac{c_e}{q_m} \quad (5)$$

Where C_e is the equilibrium MB concentration (mg/L), q_e(mg/g) is the amount of MB adsorbed at equilibrium, q_m(mg/g) is the saturated monolayer sorption capacity (also the maximal adsorption capacity), and *b* the capacity of adsorption in a saturated single layer. The isotherm parameters can be determined by plotting C_e/q_e vs. C_e (Fig.8(a)).

The Freundlich model, applied to heterogeneous surfaces, gives the dye concentration on the adsorbent surface and is given by:

$$\ln q_e = \ln K_f + \frac{1}{n} \ln c_e \quad (6)$$

Where q_e is the amount of MB adsorbed (mg/g) and C_e is the equilibrium concentration of *MB* (mg/L); K_F and *n* are the Freundlich constants, characteristic of the adsorbent/MB system, they can be determined by fitting data and which indicate the capacity and intensity of the adsorption. Fig.8(b) shows the Freundlich model for MB adsorption. The plot ln q_e vs. ln C_e is linear with a slope of 1/n and an intercept of ln K_f.

The Temkin isotherm assumes that the adsorption heat decreases with the coverage as a result of the interaction between adsorbate/adsorbent. It is characterized by a uniform distribution of binding energies, with a maximum energy and low interaction adsorbent/adsorbate. The linearized form is expressed by the following equation:

$$q_e = B \ln A_t + B \ln C_e \quad (7)$$

Where $B = \frac{RT}{b_t}$, b_t is the Temkin constant (J/mol) related to adsorption heat, and A_t the isotherm constant (L/g). The Temkin isotherm is represented by a straight line of q_e to $\ln C_e$, as shown in Fig.8(c).

All constants of the three isotherm models are reported in Table 2. According to their correlation coefficients (R^2), it seems that the Langmuir isotherm gives the best fit for the MB adsorption onto the NaY zeolites. This result

Table 2: Langmuir, Freundlich and Temkin isotherm models constants (S/L = 2 g/L, pH = 6, C_o = 10–100 mg/L and T = 25°C).

Langmuir			Freundlich			Temkin		
q_m(mg/g)	b (L/mg)	R^2	K_F (mg/g)	n	R^2	b_T(J/mol)	A_T (L/g)	R^2
6.5530	0.4276	0.9934	3.7091	8.1633	0.9409	0.5017	2397.40	0.8769

Table 3: Dimensionless constant RL of the adsorption of BM onto NaY zeolite.

C_o (mg/L)	10	20	50	75	100
R_L	0.1895	0.1047	0.0447	0.0302	0.0228

suggests that the adsorption of MB onto the surface of NaY takes place as monolayer adsorption with a favorable process. According to Langmuir model, we can express a dimensionless constant (R_L) to verify the favorability of the adsorption process and which is defined by:

$$R_L = \frac{1}{1 + bC_0} \quad (8)$$

The adsorption process can be irreversible (R_L = 0), favorable (0<R_L<1), linear (R_L=1), or unfavorable (R_L > 1) [16-18]. From Table 3, the calculated values of R_L indicated that the adsorption of MB onto NaY zeolite was favorable in all concentrations.

Kinetics studies

The kinetic study is important for the adsorption, it gives the rate of dye removal from aqueous solutions and provides data for understanding the mechanism as well as the efficiency of the adsorption process. The kinetic which governs the adsorption was studied by fitting the pseudo-first and pseudo-second-order models to the experimental data.

Lagergren pseudo first order and pseudo second order

The model is applied to the experimental data to describe the kinetic of MB adsorption [41, 48]:

$$\frac{dq}{dt} = k_1 (q_e - q_t) \quad (9)$$

Where q_e and q_t are the amounts of adsorbed MB onto the NaY (mg/g) at equilibrium and at time *t*, respectively, and k_1 the rate constant of the first-order adsorption (min^{-1}). The integrated form of Eq. (9) can be written as follows:

$$\ln (q_e - q_t) = \ln q_e - k_1 t \quad (10)$$

The *k1* values are considered as mass transfer coefficient in the adsorption, are determined from the straight lines of $\ln(q_e - q_t)$ vs. t (Fig.9(a)); the obtained R^2 values are relatively small. Hence, the pseudo-first-order model does not describe the adsorption kinetic of MB onto NaY zeolite, the data are listed in Table 4.

The pseudo-second-order kinetic model was applied to the experimental data to describe the kinetics of MB sorption [23, 49]. The model can be expressed as:

$$\frac{dq_t}{dt} = k_2 (q_2 - q_t)^2 \quad (11)$$

Where K_2 (g/mg/min) is the rate constant of the second-order adsorption. The integrated form of Eq. (11) is given below.

$$\frac{1}{d_t} = \frac{1}{k_2 q_e^2} + \frac{t}{d_e} \quad (12)$$

The plot of t/q_t versus *t* gives a straight line (Fig.9(b)), with a high correlation coefficient of (R^2= 0.9985), indicating that the pseudo-second-order is well suited to describe the MB adsorption on the NaY zeolite surface. In addition, the calculated values of $q_{e(cal)}$ agree and are very close to those determined experimentally as shown in Table 4. Otherwise, a decrease in the rate constant k_2 of the second-order adsorption with the increase of the MB concentration can be explained probably by the solute-solute interactions [49].

Photo-degradation experiments

Adsorption is a simple and inexpensive alternative for pollutant removal but loses its efficiency at small concentrations and often does not respect the limits imposed by the water standards. In this respect, photocatalytic oxidation represents an elegant strategy that can take over; it works under mild conditions and

Table 4: Pseudo-first-order and pseudo-second-order Kinetic parameters for the adsorption of MB onto NaY.

		Pseudo first-order			Pseudo second-order		
MB (mg/L)	$q_{e(exp)}$ (mg/g)	$q_{e(cal)}$ (mg/g)	$K_1 \times 10^2$ (min^{-1})	R^2	$q_{e(cal)}$ (mg/g)	$K_2 \times 10^2$ (min^{-1})	R^2
10	4.4550	1.8970	5.3	0.9215	4.4247	6.30	0.9995
20	4.7032	4.1260	7.3	0.9771	5.1098	1.55	0.9868
50	5.6871	7.3760	4.1	0.9111	7.0472	0.41	0.9444
100	7.9803	6.1480	4.0	0.9936	7.7881	0.74	0.9967

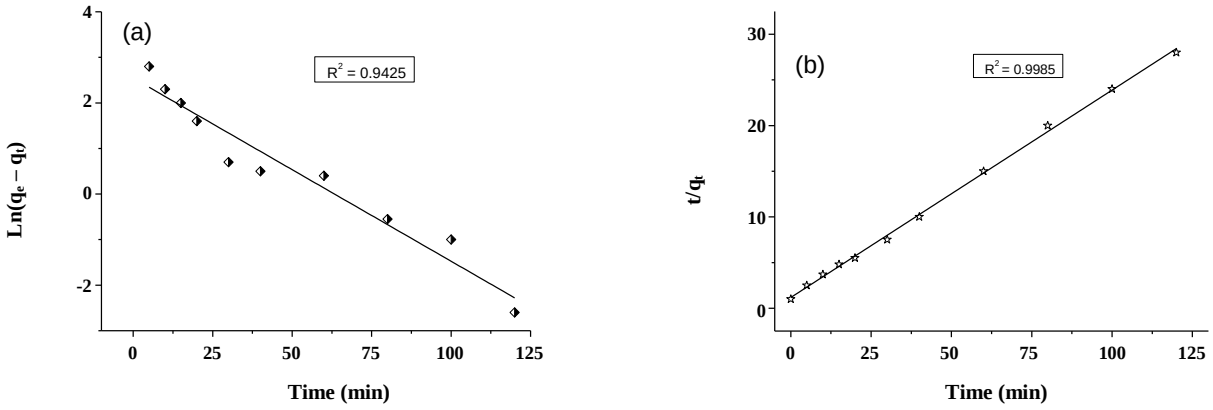

Fig. 9: (a) Pseudo-first-order and (b) pseudo-second-order plots for MB adsorption onto NaY zeolite (S/L = 2 g/L, pH = 6, C_o = 10 mg/L and T = 25°C).

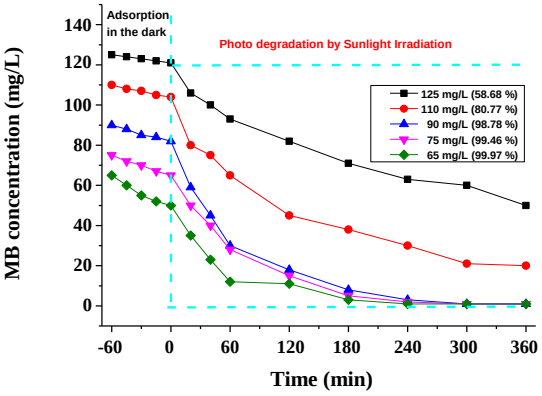

Fig. 10: Adsorption in the dark and photodegradation by sunlight irradiation of MB dye onto TiO_2/NaY for different residual concentrations (S/L = 2 g/L, pH = 6 and T = 25°C).

has been widely used for water treatment [42, 50]. Wastewaters containing dyes in the range (50-125 mg/L) can be suitably treated by photocatalysis.

In this regard, adsorption is a preamble to photocatalysis and it has been found that the adsorbed molecules are the results of the decolorization of MB residual concentration solutions using photocatalysts under UV irradiation compared to dark adsorption (Fig.10). Because of the extended surface area of NaY, we assume that the discoloration is caused only by MB adsorption onto NaY. However, the results of the NaY zeolite used with photocatalysts under sunlight irradiation rejected our assumption. The elimination process by adsorption requires a long time and the degradation cannot be completed.

The performance of supported catalysts is related to the photo carriers with the MB molecules. Dispersion of the catalyst over the TiO_2/NaY zeolite prevents aggregation of the particles and the light scattering while increasing the photo-catalytic activity by increasing the specific surface area.

However, good dispersion of TiO_2 increases the active sites, and the degradation rate of pollutants becomes faster. Furthermore, the strong electrostatic field in the TiO_2/NaY zeolite framework can effectively separate the electron/hole (e^-/h^+) pairs produced by photo-excitation of TiO_2 under UV light, thus resulting in a low recombination rate and a higher photo-degradation efficiency.

Previous work on the photodegradation of orange acid 61 on TiO_2 has shown the effectiveness of this catalyst [11]. The conduction band of TiO_2 deriving from Ti^{4+}: *4 S* orbital, is well positioned with respect to $O_2/O_2^{\bullet}$ level and should lead to oxidation of MB upon UV light because of the band bending at the interface TiO_2/MB solution. *Mekatel et al.* [11] have reported the potential of the conduction band of TiO_2 (E_{CB} = - 0.65 V) is below that of $O_2/O_2^{\bullet-}$ couple (- 0.5) and the electrons generate free radicals O_2^- responsible for the degradation of dyes. The holes $OH^{\bullet}$ are formed in the valence band and both radicals $O_2^{\bullet-}$ /$OH^{\bullet}$ are involved in the interfacial reactions:

$$TiO_2 + hn(l > 400nm) \rightarrow h^+_{VB} + e^-_{CB} \quad (13)$$

$$e^-_{CB} + O_2 \rightarrow O_2^{\bullet-} \quad (14)$$

$$h^+_{VB} + H_2O \rightarrow OH^{\bullet} + H^+ \quad (15)$$

$$H_2O + O_2 + e^-_{CB} \rightarrow H_2O_2 + OH^- \quad (16)$$

$$OH^{\bullet} + O_2^{\bullet-} + MB\ dye \rightarrow CO_2 + H_2O \quad (17)$$

$$MB\ Dye + HO^{\bullet} \rightarrow degradation\ products \quad (18)$$

$$MB\ Dye + h^+_{VB} \rightarrow oxidation\ products \quad (19)$$

$$MB\ Dye + e^-_{CB} \rightarrow reductionproducts \quad (20)$$

The reaction (Eq.(15)) favors the separation of (e^-/h^+) pairs and prevents the recombination process. The decrease of the absorbance at 665 nm during the photocatalysis with irradiation time was observed and due probably to the MB dye. The oxidation potential of OH^- and its non-selectivity allows the degradation conversion. 94% of MB dye (50 mg/L), 92.30% of MB dye (65 mg/L), 90.24% of MB dye (82 mg/L), 63.46% of MB dye (104 mg/L), and 41.32% of MB dye (121 mg/L) after 180 min of exposure to sunlight are oxidized (Fig.10). At low concentrations, 76% of MB dye are eliminated after 60 min and at high concentrations, 23 to 38% of dye are photo degraded. After 240 min, the remaining concentration of MB is oxidized (99.97%) on illuminated TiO_2 by $^{\bullet}OH$ and $O_2^{\bullet-}$ radicals owing to the suitable positions of valence and conduction bands.

Our results confirm the relationship between the adsorption and the photocatalytic activity, as the photo-degradation of organic pollutants occurs after their adsorption on the surface.

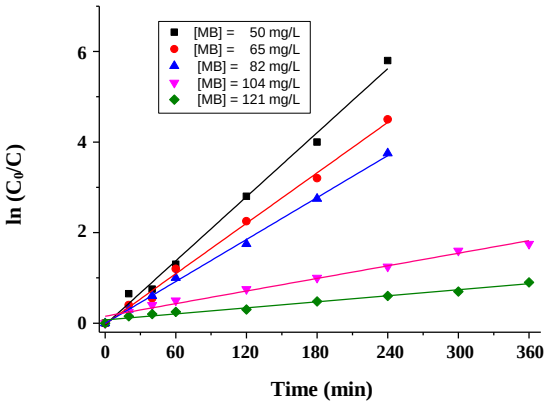

Fig. 11: Photocatalytic degradation kinetics of MB dye onto TiO_2/NaY for different residual concentrations (S/L = 2 g/L, pH = 6 and T = 25°C).

Kinetic study

The kinetics of the degradation of MB dye was investigated using the Langmuir-Hinshelwood model (LH). The kinetic parameters have been determined by the following equations [51]:

$$r = -\frac{dC}{dt} = K_{app} C_0 \quad (21)$$

$$\ln\left(\frac{C_0}{C}\right) = K_{app} t \quad (22)$$

$$K_{app} = K_r K_s \quad (23)$$

Where r (min^{-1}): apparent initial rate, C_0 : MB dye concentration, K_s (L/mg): LH adsorption equilibrium constant, and K_r (mg/L.min): rate constant. The plot of (Eq. (22)) gives the K_{app} values for photodegradation of MB dye (Fig.11) and Table 5. The values of constants (K_s) and (K_r) are determined by plotting ($1/K_{app}$) as a function of C_0 (Fig.12).

The results of Table 5 show the values of the apparent kinetic constants and confirm that they are dependent on the MB dye concentrations, indicating that MB photocatalytic degradation follows a first-order kinetic of the Langmuir-Hinshelwood. The apparent kinetic constants decrease with increasing concentration, indicating also that the LH model is valid and the reaction of photodegradation takes place in the TiO_2/NaY-liquid interface.

CONCLUSIONS

Highly active surface NaY zeolite was impregnated by a sunlight-sensitive catalyst, TiO_2 to study the photo-catalytic

Table 5: Kinetic parameters of MB dye photo degradation onto TiO_2/NaY.

C_0(mg/L)	K_{app} (min^{-1})	R^2	K_r (mg/L.min)	K_s (L/mg)
50	0.0236	0.9931	0. 1996	0.1182
65	0.0186	0.9953		
82	0.0154	0.9980		
104	0.0046	0.9837		
121	0.0022	0.9770		

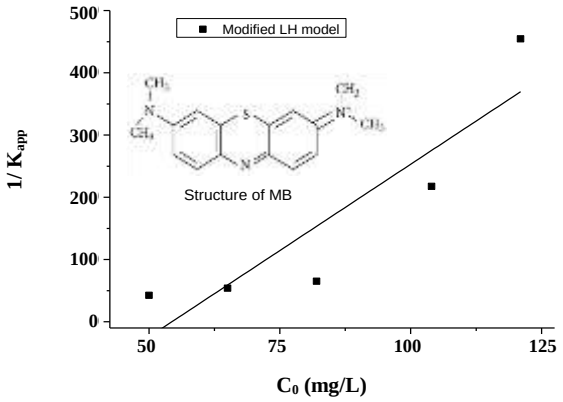

Fig. 12: Plot of $1/K_{app}$ as a function of C_0 according to the modified Langmuir–Hinshelwood model.

degradation of methylene blue in aqueous solutions. XRD, SEM, and FT-IR characterization show higher dispersion of TiO_2 particles in the NaY zeolite structure.

The MB adsorption process onto NaY zeolite parameters were optimized ([MB] = 10 mg/L, pH = 6, S/L = 2 mg/L and T = 25°C). High performance towards MB dye was achieved using NaY with a percentage adsorption of 88% and an adsorption capacity of 6.55 mg/g. The equilibrium study reveals that Langmuir isotherm has a better fitting indicating a monolayer coverage of MB dye onto NaY surface. The positive value of ΔH° highlighted both the endothermic and physical process natures.

The ΔG° and ΔS° values indicated the spontaneity and affinity of the NaY toward MB dye. The kinetic investigation showed that pseudo-second-order adsorption is predominant. The efficiency of TiO_2 is directly associated with the NaY zeolite photo-degradation of MB dye. The photo-degradation of the MB not adsorbed by NaY was successfully carried out on the TiO_2/NaY catalyst under sunlight for concentrations ranging from 50 to 121 mg/L. The kinetic according to the Langmuir-Hinshelwood model followed first-order kinetic and the determined apparent kinetic constants indicated its validity.

From all these conclusions, we can deduce that the dye degradation by TiO_2 deposited on NaY zeolite surface is very attractive for environmental application.

Acknowledgments

Our big gratitude to the General Direction of Scientific Research and Technological Development (DGRSDT) and the Thematic Research Agency in Science and Technology (ATRST) of the Ministry of Higher Education and Scientific Research of the Democratic Republic of Algeria.

Received : Jun. 4, 2021 ; Accepted : Aug. 2, 2021

REFERENCES

[1] Parisi M., Fatarella E., Spinelli D., Pogni R., Basosi R., Environmental Impact Assessment of an Eco-Efficient Production for Coloured Textiles, *J. Clean. Prod*., **108**: 514-524 (2015).

[2] Natarajan S., Bajaj H., Tayade R., Recent Advances Based on the Synergetic Effect of Adsorption for Removal of Dyes From Waste Water Using Photocatalytic Process, *Int. J. Environ. Sci*., **65**: 201-222 (2018).

[3] Bethi B., Sonawane S., Bhanvase B., Gumfekar S., Nanomaterials-Based Advanced Oxidation Processes for Wastewater Treatment: a Review, *Chem. Eng. Process*., **109**: 178-189 (2016).

[4] Mittersteiner M., Schmitz F., Barcellos I., Reuse of Dye-Colored Water Post-Treated with Industrial Waste: Its Adsorption kinetics and Evaluation of Method Efficiency in Cotton Fabric Dyeing, *J. Water. Process Eng*., **1**: 181-187 (2017).

[5] Yeap K., Teng T., Poh B., Morad N., Lee K., Preparation and Characterization of Coagulation/ Flocculation Behavior of a Novel Inorganic–Organic Hybrid Polymer for Reactive and Disperse Dyes removal, *Chem. Eng. J*., 243: **305**-314 (2014).

[6] Brillas E., Martínez-Huitle C., Decontamination of Wastewaters Containing Synthetic Organic Dyes by Electrochemical Methods. An Updated Review, *Appl. Catal. B-Environ*., **166**: 603-643 (2015).

[7] Borges G., Silva L., Penido J., de Lemos L., Mageste A., Rodrigues G., A Method for Dye Extraction Using an Aqueous Two-Phase System: Effect of Co-Occurrence of Contaminants in Textile Industry Wastewater, *J. Environ. Manage*., **183**: 196-203 (2016).

[8] Forgacs E., Cserhati T., Oros G., Removal of Synthetic Dyes From WasteWaters: A Review, *Environ. Int*., **30**: 953-971 (2004).

[9] Mekatel H., Amokrane S., Aid A., Nibou D., Trari M., Adsorption of Methyl Orange on Nanoparticles of a Synthetic Zeolite NaA/CuO, *CR. Chim*., **18**: 336-344 (2015).

[10] Grčić I., Papić S., Mesec D., Koprivanac N., Vujević D., The Kinetics and Efficiency of UV Assisted Advanced Oxidation of Various Types of Commercial Organic Dyes in Water, *J. Photochem. Photobiol A: Chem*., **273**: 49-58 (2014).

[11] Mekatel EH., Amorkrane S., Trari M., Nibou D., Dahdouh N., Ladjali S., Combined Adsorption/ Photocatalysis Process for the Decolorization of Acid Orange 61, *Arab. J. Scie. Eng.*, **44(6)**: 5311-5322 (2019).

[12] Belaissa Y., Nibou D., Assadi A., Bellal B., Trari M., A New Hetero-Junction P-CuO/n-ZnO for the Removal of Amoxicillin by Photocatalysis under Solar Irradiation, *J. Taiwan. Inst. Chem. Eng*., **68**: 254-265 (2016).

[13] Soltani T., Entezari H., Photolysis and Photocatalysis of Methylene Blue by Ferrite Bismuth Nanoparticles Under Sunlight Irradiation, *J. Mol. Catal. A-Chem*., **377**: 197-203 (2013).

[14] Borges M., Sierra M., Cuevas E., García R., Esparza P., Photocatalysis with Solar Energy: Sunlight-Responsive Photocatalyst Based on TiO_2 Loaded on a Natural Material for Wastewater Treatment, *Solar. Eng*., **135**: 527-535 (2016).

[15] Yonli A., Batonneau-Gener I., J. Koulidiati, Adsorptive Removal of α-Endosulfan from Water by Hydrophobic Zeolites. An Isothermal Study, *J. Hazard. Mater*., **203**: 357-362 (2012).

[16] Nibou D., Mekatel H., Amokrane S., Barkat M., Trari M., Adsorption of Zn^{2+} Ions onto NaA and NaX Zeolites: Kinetic, Equilibrium and Thermodynamic Studies, *J. Hazard. Mater.*, **173**: 637-646 (2010).

[17] Barkat M., Nibou D., Amokrane S., Chegrouche S., Mellah A., Uranium (VI) Adsorption on Synthesized 4A and P1 Zeolites: Equilibrium, Kinetic, and Thermodynamic Studies, *Com. Rend. Chim.*, **18(3)**: 261-269 (2015).

[18] Ferhat D., Nibou D., Mekatel E.H., Amokrane S., Adsorption of Ni^{2+} Ions onto NaX and NaY Zeolites: Equilibrium, Kinetic, Intra Crystalline Diffusion and Thermodynamic Studies, *Iran. J. Chem. Chem. Eng. (IJCCE)*, **38 (6)**: 63-81(2019).

[19] Nibou D., Amokrane S., Lebaili N., Use of NaX Porous Materials in the Recovery of Iron Ions, *Desalination* **250** (**1**), 459-462 (2010).

[20] Benmessaoud A. Nibou D., Mekatel E.H., Amokrane S., A Comparative Study of the Linear and Non-Linear Methods for Determination of the Optimum Equilibrium Isotherm for Adsorption of Pb^{2+} Ions onto Algerian Treated Clay, *Iran. J. Chem. Chem. Eng. (IJCCE)*, **39 (4)**: 153-171 (2020).

[21]Mekatel E.H., Trari M., Nibou D., Ibtissam S., Amorkrane S., Preparation and Characterization of α-Fe_2O_3 Supported Clay as a Novel Photocatalyst for Hydrogen Evolution, *Inter. J. Hydro Ener.*, **44 (21):** 10309-10315 (2019).

[22] Aid A., Amokrane S., Nibou D., Mekatel E., Trari M., Hulea V., Modeling Biosorption of Cr (VI) onto Ulva Compressa L. from Aqueous Solutions, *Wat. Sci. Tech.*, **77(1)**: 60-69 (2018).

[23] Ladjali S., Amokrane S., Mekatel E.H., Nibou D.**,** Adsorption of Cr(VI) on Stipa Tenacissima L (Alfa): Characteristics, Kinetics and Thermodynamic Studies, *J. Sep. Sci. Tech.*, **54(6)**: 876-887 (2019).

[24] Chen Y., Zhai S., Liu N., Song Y., An Q., Song X., Dye Removal of Activated Carbons Prepared from NaOH-Pretreated Rice Husks by Low-Temperature Solution-Processed Carbonization and H_3PO_4 Activation, *Bioresour. Technol*., **144**: 401-409 (2013).

[25] Haddad D., Mellah A., Nibou D., Khemaissia S., Promising Enhancement in the Removal of Uranium Ions by Surface-Modified Activated Carbons: Kinetic and Equilibrium Studies, *J. Environ. Eng.*, **144(5)**: 04018027 (2018)

[26] Nibou D. and Amokrane S., Catalytic Performances of Exchanged Y Faujasites by Ce^{3+}, La^{3+}, UO_2^{2+}, Co^{2+}, Sr^{2+}, Pb^{2+}, Tl^{+} and NH_4^{+} Cations in Toluene Dismutation Reaction, *Compt. Rend. Chim.*, 1**3(5)**: 527-537 (2010).

[27] Nibou D. and Amokrane S., Dependence Between The Activity and Selectivity Of NaLaY and NaCeY Catalysts in the Catalytic Disproportionation of Toluene, *Stud. Surf. Scie. Catal. Series*. **158** B: 1645-1652 (2005).

[28] Nibou D., Azzouz A., Dumitriu E., Bilba V., Comparative Study on the Effect of Introducing the Uranyl Ion and Various Multivalent Cations into Y-Faujasite and an Algerian Bentonite, *Rev. Roum. Chim.* **39(9)**: 1099-1108 (1994).

[29] Azzouz A., Nibou D., Abbad A., Achache M., Hydrocarbons Conversions over Y-Zeolite Used in Uranium ore Wastes Treatment Activity and Selectivity of Y-Faujasite Modified by Uranyl Ions in the Catalytic Disproportionation of Toluene, *Appl. Catal. (General A)*, **79(1)**: 19-28 (1991).

[30] Amokrane S., Rebiai R., Lebaili S., Nibou D., Marcon G., Selective synthesis of Monooctylamines by Ammonia Alkylation with Octanol Using NaY, ZSM-5 SAPO-5, SAPO-11, SAPO-31, SAPO-34, *Study Surf. Scie. Catal. Series* **135**: 230 (2001).

[31] Azzouz A., Nibou D., Abbad B., Achache M., Catalytic Amination of Octanol in Gas Phase. Action of Uranyle Ions over the Catalytic Activity of Y Faujasite, *J. Mole.Catal.* **68 (2)**: 187-197 (1991)

[32] Breck D.W., Zeolite Molecular Sieves-Structure Chemistry and Use, Wiley Interscience, New York (1974).

[33] Krobba A., Nibou D., Amokrane S., Mekatel H., Adsorption of Copper (II) onto Molecular Sieves NaY, *Desal. Wat. Treat.*, **37**: 1–7 (2012).

[34] Houhoune F., Nibou D., Amokrane S., Barkat M., Modelling and Adsorption Studies of Removal Uranium (VI) Ions on Synthesised Zeolite NaY, *Des. Wat. Treat.*, **51 (28-30)**: 5583-5591 (2013).

[35] Amokrane S., Rebiai R., Nibou D., Behaviour of Zeolite A, Faujasites X and Y Molecular Sieves in Nitrogen Gas Adsorption, *J. Appl. Sci.*, **7**: 1985-1988 (2007).

[36] Baerlicher C., Meier W.M., Olson D.H., "Atlas of Zeolite Framework Types", 5th Revised Ed. Elsevier, Amesterdam (2001).

[37] Tayade R., Kulkarni R., Jasra R., Enhanced Photocatalytic Activity of TiO_2-Coated NaY and HY Zeolites for the Degradation of Methylene Blue in Water, *Ind. Eng. Chem. Res.*, **46**: 369-376 (2007).

[38] M.M.J. Traecy et J.B. Higging, "Collection of Simulated X Patterns for Zeolites". 4th Revised Ed. Elsevier, Amesterdam. (2001).

[39] Shirani M., Semnani A., Haddadi H., Habibollahi S., Optimization of Simultaneous Removal of Methylene Blue, Crystal Violet, and Fuchsine from Aqueous Solutions by Magnetic NaY Zeolite Composite, *Water. Air. Soil. Poll.*, **225**: 2054 (2014).

[40] Zendehdel M., Kalateh Z., Alikhani H., Efficiency Evaluation of NaY Zeolite and TiO_2/NaY Zeolite in Removal of Methylene Blue Dye from Aqueous Solutions, *J. Environ. Health. Sci. Eng.*, **8**: 265 (2011).

[41] Aysan H., Edebali S., Ozdemir C., Karakaya M.C.k., Karakaya N., Use of Chabazite, a Naturally Abundant Zeolite, for The Investigation of The Adsorption Kinetics and Mechanism of Methylene Blue Dye, *Micropor. Mesopor. Mat.*, **235**: 78-86 (2016).

[42] Abkenar S.D., Ganjali M.R., Hossieni M., Karimi M.S., Application of Copper Vanadate Nanoparticles for Removal of Methylene Blue from Aqueous Solution: Kinetics, Equilibrium, and Thermodynamic Studies, *Iran. J. Chem. Chem. Eng. (IJCCE)*, **38(6)**: 83-92 (2019)

[43] EL-Mekkawi D., Ibrahim F., Selim M., Removal of Methylene Blue from Water Using Zeolites Prepared from Egyptian Kaolins Collected from Different Sources, *J. Environ. Chem. Eng.*, **4:** 1417-1422 (2016).

[44] Mekatel E.H., Nibou D., Trari M., Amokrane S., Dahdouh N., Removal of Maxilon Red by Adsorption and Photocatalysis: Optimum Conditions, Equilibrium and Kinetic Studies, *Iran. J. Chem. Chem. Eng. (IJCCE)*, **40 (1)**: 93-110 (2021).

[45] Malekbala M., Khan M., Hosseini S., Abdullah L., Choong T., Adsorption/Desorption of Cationic Dye on Surfactant Modified Mesoporous Carbon Coated Monolith: Equilibrium, Kinetic and Thermodynamic Studies, *J. Ind. Eng. Chem.*, **21**: 369-377 (2015).

[46] Tseng R., Tseng S., Pore Structure and Adsorption Performance of The KOH-Activated Carbons Prepared from Corncob, *J. Colloid. Interface. Sci.*, **287**: 428-437 (2005).

[47] Senthilkumaar S., Kalaamani P., Porkodi K., Varadarajan P., Subburaam C., Adsorption of Dissolved Reactive Red Dye from Aqueous Phase Onto Activated Carbon Prepared from Agricultural Waste, *Bioresour. Technol*., **97**: 1618-1625 (2006).

[48] Mall I., Srivastava V., Agarwal N., Removal of Orange-G and Methyl Violet Dyes by Adsorption Onto Bagasse Fly Ash—Kinetic Study and Equilibrium Isotherm Analyses, *Dyes. Pigm*., **69**: 210-223 (2006).

[49] Lin L., Lin Y., Li C., Wu D., Kong H., Synthesis of Zeolite/Hydrous Metal Oxide Composites from Coal Fly Ash as Efficient Adsorbents for Removal of Methylene Blue from Water, *Int. J. Miner. Process*., **14**: 32-40 (2016).

[50] Chong M., Jin B., Chow C., Saint C., Recent Developments in Photocatalytic Water Treatment Technology: a Review, *Water. Res*, **44**: 2997-3027 (2010).

[51] Faraji H., Mohamadi A.A., Arezomand H.R.S., Mahvi A.H., Kinetics and Equilibrium Studies of the Removal of Blue Basic 41 and Methylene Blue from Aqueous Solution Using Rice Stems, *Iran. J. Chem. Chem. Eng. (IJCCE),* **34(3)**: 33-42 (2015).